Am J Physiol Regulatory Integrative Comp Physiol
280: R1844–R1852, 2001.

Gill Na^+-K^+-$2Cl^-$ cotransporter abundance and location in Atlantic salmon: effects of seawater and smolting

RYAN M. PELIS, JOSEPH ZYDLEWSKI, AND STEPHEN D. McCORMICK
Conte Anadromous Fish Research Center, Biological Resources Division, United States Geological Survey, Turners Falls 01376, and Organismic and Evolutionary Biology Program, University of Massachusetts, Amherst, Massachusetts 01003

Received 13 October 2000; accepted in final form 24 January 2001

Pelis, Ryan M., Joseph Zydlewski, and Stephen D. McCormick. Gill Na^+-K^+-$2Cl^-$ cotransporter abundance and location in Atlantic salmon: effects of seawater and smolting. *Am J Physiol Regulatory Integrative Comp Physiol* 280: R1844–R1852, 2001.—Na^+-K^+-$2Cl^-$ cotransporter abundance and location was examined in the gills of Atlantic salmon (*Salmo salar*) during seawater acclimation and smolting. Western blots revealed three bands centered at 285, 160, and 120 kDa. The Na^+-K^+-$2Cl^-$ cotransporter was colocalized with Na^+-K^+-ATPase to chloride cells on both the primary filament and secondary lamellae. Parr acclimated to 30 parts per thousand seawater had increased gill Na^+-K^+-$2Cl^-$ cotransporter abundance, large and numerous Na^+-K^+-$2Cl^-$ cotransporter immunoreactive chloride cells on the primary filament, and reduced numbers on the secondary lamellae. Gill Na^+-K^+-$2Cl^-$ cotransporter levels were low in presmolts (February) and increased 3.3-fold in smolts (May), coincident with elevated seawater tolerance. Cotransporter levels decreased below presmolt values in postsmolts in freshwater (June). The size and number of immunoreactive chloride cells on the primary filament increased threefold during smolting and decreased in postsmolts. Gill Na^+-K^+-ATPase activity and Na^+-K^+-$2Cl^-$ cotransporter abundance increased in parallel during both seawater acclimation and smolting. These data indicate a direct role of the Na^+-K^+-$2Cl^-$ cotransporter in salt secretion by gill chloride cells of teleost fish.

Salmo salar; chloride cells; teleost; osmoregulation; Na^+-K^+-ATPase

THE NA^+-K^+-$2CL^-$ COTRANSPORTER is an integral membrane protein found in numerous epithelia where it functions in cell volume regulation and ion transport (4, 10, 23, 25, 42). The Na^+-K^+-$2Cl^-$ cotransporter is widely distributed among many different species of vertebrates, including the rat, duck, rabbit, dog, cow, and human (23). Among fish, the Na^+-K^+-$2Cl^-$ cotransporter has been shown to be present within the intestinal epithelium of the winter flounder, *Pseudopleuronectes americanus* (9, 33, 34, 39), and the rectal gland of the spiny dogfish, *Squalus acanthias* (22).

Pharmacological studies using *p*-sulfamoylbenzoic acid derivatives ("loop diuretics"; e.g., furosemide, bumetanide, and benzmetanide) indicate that the Na^+-K^+-$2Cl^-$ cotransporter is involved in salt secretion by marine teleosts. The short-circuit current of the opercular membrane is a direct measure of chloride secretion and is inhibited by loop diuretics in seawater-acclimated killifish, *Fundulus heteroclitus* (6, 16). Furthermore, the transepithelial potential of the flounder gill is reduced after exposure to furosemide (2).

Chloride cells have been shown to be the site of chloride secretion in the gills of seawater-acclimated teleosts (8). Current models of chloride cell function in euryhaline teleosts indicate that these cells have unique functions and compositions of transporters depending on the salinity of the surrounding environment (see review, Ref. 7). The studies cited above indicate that a loop diuretic-sensitive cotransporter is an integral part of the salt-secreting mechanism of the chloride cell. In the current model of the seawater chloride cell, basolaterally located Na^+-K^+-ATPase creates a sodium gradient that is used by a basolateral Na^+-K^+-$2Cl^-$ cotransporter to transport sodium, potassium, and two chloride ions into the cell. Once inside the cell, chloride ions leave down their electrochemical gradient through an apical Cl^- channel, whereas sodium is transported back into the basal lamina via Na^+-K^+-ATPase. The buildup of sodium in the basal lamina allows it to exit into the external media on a paracellular pathway.

Of these three major transporters involved in salt secretion, only Na^+-K^+-ATPase has been definitively localized to chloride cells (13, 17, 26, 41). Gill Na^+-K^+-ATPase activity has been found to increase during the seawater acclimation of teleosts (5, 14), including Atlantic salmon, *Salmo salar* (38). Although salt secretion through chloride cells in teleosts likely involves the Na^+-K^+-$2Cl^-$ cotransporter, direct evidence for the presence and localization of this protein in chloride cells is conspicuously lacking. In addition, there is no information on the regulation of this protein by environmental salinity or developmental events.

The study of anadromous fish provides the opportunity to probe the effects of environmental salinity and

Address for reprint requests and other correspondence: R. M. Pelis, Univ. of Connecticut, Physiology and Neurobiology, U-4156, BBS #4, Rm. 021, 3107 Horsebarn Hill Rd., Storrs, CT 06269-4156 (E-mail: ryan.pelis@uconn.edu).

The costs of publication of this article were defrayed in part by the payment of page charges. The article must therefore be hereby marked "*advertisement*" in accordance with 18 U.S.C. Section 1734 solely to indicate this fact.

the development of seawater tolerance on chloride cell-associated proteins. Anadromy is a life history strategy that includes a freshwater and marine phase. This strategy is exemplified by Atlantic salmon, which hatch and remain in freshwater for several years as parr before seaward migration. The time preceding and during migration is a critical developmental period called "smolting." Smolting includes a number of behavioral, morphological, and physiological changes that are preparatory for seawater entry (12). These changes are incomplete in juveniles before the period of downstream migration (presmolts) and are reversed in salmon that do not successfully reach the ocean (postsmolts).

Physiological changes occurring in the gill, kidney, gut, and bladder are responsible for increased salinity tolerance among smolts before seaward migration (30). Chloride cell size and density have been found to increase after the acclimation of Atlantic salmon to seawater and during smolting (18). Numerous studies have found increased gill Na^+-K^+-ATPase activity during smolting and seawater acclimation (21, 31, 37). These data suggest a direct relationship between increased gill Na^+-K^+-ATPase activity and increased hypoosmoregulatory ability of smolts.

If the Na^+-K^+-$2Cl^-$ cotransporter is present within the gills of Atlantic salmon and is important for seawater tolerance, then it is likely that this protein would also be upregulated during seawater acclimation and smolting. The current study was designed to determine whether the Na^+-K^+-$2Cl^-$ cotransporter is present in gill chloride cells of Atlantic salmon. SDS-PAGE and Western blotting were used to characterize and quantify the gill Na^+-K^+-$2Cl^-$ cotransporter. Immunocytochemistry was used to localize the Na^+-K^+-$2Cl^-$ cotransporter to cells in the gill and to determine changes in immunoreactive cell number, size, shape, and staining intensity. Changes in the quantity and location of this protein during seawater acclimation and smolting were determined using the T4 monoclonal antibody (23). The results of these experiments provide direct evidence that the Na^+-K^+-$2Cl^-$ cotransporter is present within gill chloride cells of teleost fish. The upregulation of the Na^+-K^+-$2Cl^-$ cotransporter during seawater acclimation and smolting provides strong support for a crucial role of this protein in the mechanism of ion secretion.

METHODS

Animals and experimental protocols. To monitor the Na^+-K^+-$2Cl^-$ cotransporter in the gill during seawater acclimation, Atlantic salmon parr were acclimated to a 1,100-liter flow-through circular tank with temperatures held constant at 10 ± 0.5°C for 2 wk. On the basis of their size (<12 cm fork length), these fish were not expected to smolt. On January 31, 2000, one-half of the fish (n = 16) were moved into an identical tank in a closed recirculating system maintained at 10 ± 0.5°C and 15 parts per thousand (ppt) salinity. On February 14 and 28, the salinity was increased to 25 and 30 ppt, respectively. Freshwater controls (n = 16) and seawater-acclimated fish (n = 16) were sampled on March 7, 2000. All fish were maintained on simulated natural photoperiod and fed commercial Atlantic salmon diet (Zeigler Brothers) daily throughout the study period.

To monitor the Na^+-K^+-$2Cl^-$ cotransporter in the gill before, during, and after smolting, juvenile Atlantic salmon were transferred in January 2000 into a 1,100-liter flow-through circular tank with fresh water supplied from the Connecticut River. These fish were expected to smolt based on their size (>14 cm fork length). Fish were maintained under simulated natural photoperiod and within 0.5°C of ambient river temperatures and fed commercial salmon diet daily throughout the experimental period. Juvenile fish were sampled on February 16, May 9, and June 29 (n = 8). Atlantic salmon parr (<12 cm fork length) maintained under identical conditions were sampled on May 9 (n = 16) for reference. Seawater tolerance of juvenile Atlantic salmon was determined by measuring their ability to regulate plasma ions in 24-h seawater challenge tests. Twenty-four-hour seawater challenges were conducted in a 1,100-liter closed recirculating seawater system maintained at 35 ppt with temperatures ±1.0°C of ambient river temperatures. Seawater challenges were performed on March 14 (n = 7) and May 7 (n = 7). Plasma ion levels (Na^+ and Cl^-) were measured using an electrolyte analyzer (AVL Scientific).

At the time of sampling, all fish were anesthetized with 100 mg/l MS-222 (pH 7.0, 12 mM $NaHCO_3$), weighed to the nearest 0.1 g, and fork lengths were recorded. To measure gill Na^+-K^+-ATPase activity, gill biopsies (5 or 6 gill filaments) were placed in 100 μl of ice-cold SEI (in mM: 250 sucrose, 10 Na_2EDTA, and 50 imidazole) and stored at −80°C. A single gill arch from each fish was removed, plunged into fixative (80% absolute methanol-20% dimethyl sulfoxide at −20°C) and stored at −20°C for later use in immunocytochemistry. The remaining gill tissue was removed, snap-frozen on dry ice, and stored at −80°C to be later used for gel electrophoresis. For seawater-challenged juvenile Atlantic salmon, blood was drawn from the caudal blood vessels into a 1-ml ammonium heparinized syringe and centrifuged at 8,000 g for 5 min at 4°C. Plasma was separated and stored at −80°C.

Antibodies. T4 monoclonal antibodies developed against the carboxy terminus of the human colonic Na^+-K^+-$2Cl^-$ cotransporter were used as the primary antibody for the Na^+-K^+-$2Cl^-$ cotransport protein in the Atlantic salmon gill. The T4 antibody, developed by Dr. Christian Lytle and Dr. Bliss Forbush III, was obtained from the Developmental Studies Hybridoma Bank developed under the auspices of the National Institute of Child Health and Human Development and maintained by the University of Iowa, Department of Biological Sciences, Iowa City, IA 52242. This antibody was used at a concentration of 600 μg/ml for Western blots and 300 μg/ml for immunocytochemistry.

Localization of Na^+-K^+-ATPase was performed using a polyclonal antibody directed against a consensus sequence of the α-subunit (generously provided by Dr. Kazuhiro Ura, Ref. 41). This antibody was used at a dilution of 1:500 for immunocytochemistry.

For Western blotting, a peroxidase-labeled goat anti-mouse IgG, heavy and light chain (H+L) was used as the secondary antibody (2 μg/ml; Kirkegaard & Perry Laboratories, Gaithersburg, MD). For immunocytochemistry, secondary antibodies included fluorescein-labeled goat anti-rabbit IgG (H+L) and Cy3-labeled goat anti-mouse IgG, H+L (2.5 μg/ml and 2 μg/ml, respectively; Kirkegaard & Perry Laboratories) for the localization of Na^+-K^+-ATPase and the Na^+-K^+-$2Cl^-$ cotransporter, respectively.

Gill Na^+-K^+-ATPase activity. Gill Na^+-K^+-ATPase activity was measured by the method of McCormick (27). Gill tissue taken from biopsies was thawed immediately before

assay and homogenized in 125 μl of 0.1% sodium deoxycholate SEI buffer for 10–15 s. The resulting homogenate was centrifuged at 5,000 *g* for 30 s, and the supernatant was retained and assayed for Na^+-K^+-ATPase activity. Each sample of gill homogenate was plated in quadruplicates of 10 μl. Fifty microliters of salt solution (in mM: 50 imidazole, 189 NaCl, 10.5 $MgCl_2 \times 6$ H_2O, and 42 KCl) and 150 μl of assay mixture (50 mM imidazole, 2 mM phosphoenolpyruvate, 0.16 mM nicotinamide adenine dinucleotide, 0.5 mM adenosine triphosphate, 3.3 U/ml lactic dehydrogenase, and 3.6 U/ml pyruvate kinase) were added to each well. Each sample was measured four times, twice with ouabain (0.5 mM) and twice without. The kinetic assay was read at a wavelength of 340 nm with a run time of 10 min and intervals of 10 s. The difference between the kinetic reading with and without ouabain is measured as ouabain-sensitive Na^+-K^+-ATPase activity. Protein concentration of the gill homogenate was determined using the bicinchoninic acid method (BCA Protein Kit, Pierce, Rockford, IL). Na^+-K^+-ATPase activity is expressed as micromoles ADP per milligram protein per hour.

SDS-PAGE and Western blotting. SDS-PAGE and Western blotting were used to quantify the amounts of Na^+-K^+-2Cl^- cotransporter present in the gill. Frozen gill tissue was thawed, rinsed in ice-cold PBS (in mM: 137 NaCl, 2.7 KCl, 4.3 Na_2HPO_4, 1.4 KH_2PO_4 adjusted to pH 7.3), and blotted on a paper towel. Gill epithelia were cut away from the arches and placed in 10 vol of ice-cold homogenization buffer (2 mM EDTA and 30% sucrose wt/vol in PBS) along with the following protease inhibitors: 0.2 mM [4-(2-aminoethyl)benzenesulfonylfluoride HCl], 100 μM *N*-tosyl phenylalanine chloromethyl ketone, 1 μM pepstatin A, 10 μM chymostatin, 10 μM leupeptin, and 50 μM *o*-phenanthroline. Gill tissue for Atlantic salmon parr were grouped in pairs to obtain enough protein for electrophoresis. Gill tissue was homogenized at low speed using a tissue homogenizer (Tekmar; SDT-182EN fitted with a saw tooth generator) and centrifuged at 5,000 *g* for 10 min at 4°C. The resulting supernatant was centrifuged at 20,000 *g* for 10 min, and the pellet was removed to discard mitochondria and cellular debris. The supernatant was centrifuged at 48,000 *g* for 2 h at 4°C. The final pellet was resuspended in homogenization buffer, and total protein was determined using the BCA protein assay. Enrichment of the basolateral membrane, determined by measuring Na^+-K^+-ATPase activity, was 15-fold higher than the crude homogenate.

Membranes were placed in Laemmli sample buffer (250 mM Tris base, 10% glycerol wt/vol, 2% SDS wt/vol, 1% β-mercaptoethanol wt/vol, 0.05% bromophenyl blue wt/vol in deionized water adjusted to pH 6.8) and heated to 60°C for 15 min. Membranes were loaded on 7% SDS polyacrylamide gels at 50 μg of protein per lane. Gels were run overnight followed by transfer to immobilon P [polyvinylidene fluoride (PVDF)] transfer membranes (Millipore, Bedford, MA). PVDF membranes were immersed for 1.5 h in blocking buffer (7.5% nonfat dry milk and 0.1% Tween 20 wt/vol in PBS) at room temperature and were incubated overnight at 4°C in T4 primary antibody diluted in blocking buffer. PVDF membranes were washed five times in blocking buffer followed by a 2-h incubation at room temperature in peroxidase-labeled secondary antibody in blocking buffer. PVDF membranes were washed four times in blocking buffer, once in 0.1% Tween 20 (wt/vol) in PBS, and once in deionized water. Immunoreactivity was visualized using DAB buffer [1.38 mM 3,3′-diaminobenzidine tetrahydrochloride (DAB), 0.0084 mM $CoCl_2$, and 0.001% H_2O_2 wt/vol in PBS].

Digital photographs were taken immediately after incubation with DAB. Band staining intensity was measured from the digital photographs using Image calc (C. H. A. van de Lest, Dutch Asthma Foundation). To obtain staining intensity, an entire lane on a Western blot is selected, and Image calc scans the selected part of the image from top to bottom, averaging the 8-bit gray scale values that are located on each horizontal line. The average 8-bit gray scale values on each horizontal line are then summed to obtain cumulative 8-bit gray scale values for each particular band. To standardize for differences in background intensity between Western blots, the background 8-bit gray scale value was subtracted from each horizontal line average 8-bit gray scale value. Na^+-K^+-2Cl^- cotransporter abundance, as measured by staining intensity, is recorded as cumulative 8-bit gray scale.

Enzymatic deglycosylation. Enzymatic deglycosylation was performed on gill tissue from four smolts to determine the degree to which the protein isolated on Western blots was glycosylated. After isolation, plasma membranes were brought up in deglycosylation buffer (2 mM EDTA and 1% SDS wt/vol in PBS). Protein content was determined through the BCA method as described above. Enzymatic deglycosylation was accomplished by adding *N*-glycosidase-F (0.02 U/5 μg protein) to the samples and incubating at 20°C for 18 h. After deglycosylation, plasma membrane samples were electrophoresed on 7% polyacrylamide gels, blotted, and stained using the procedures mentioned previously.

Immunocytochemistry. Immunocytochemical procedures were modified from Ginns et al. (10). After fixation (80% absolute methanol-20% dimethyl sulfoxide) at −20°C, tissue was placed on ice and allowed to warm before being placed in Ringer at 4°C. The tissue was then equilibrated in cryoprotectant (30% sucrose wt/vol in Ringer) before being embedded in Histo Prep Embedding Media (Fisher Scientific). Tissue was frozen (−25°C), cryosectioned at 10 μm, placed on warm poly-L-lysine-subbed slides, and washed twice with high-salt Ringer (360 mM NaCl and 1% BSA wt/vol in Ringer). Sections were washed three times in glycine wash (50 mM glycine and 1% BSA wt/vol in Ringer) and incubated overnight in primary antibodies at 4°C (T4 and anti-Na^+-K^+-ATPase α-subunit diluted in 0.1% NaN_2 and 1% BSA wt/vol in Ringer). Both primary antibodies were used together during colocalization studies. After incubation with primary antibodies, tissue was washed five times in high-salt Ringer, incubated for 2 h at 4°C in secondary antibodies, and washed twice in Ringer before viewing. All washes were 10 min in length. Controls omitting the primary antibodies were performed and yielded no immunoreactivity. For colocalization studies, controls consisted of omitting one of each of the secondary antibodies, and no cross-reactivity was detected.

Na^+-K^+-2Cl^- cotransporter immunoreactive chloride cells on the primary filament and secondary lamellae were tallied separately. From each fish, immunoreactive chloride cells were counted from 10 sagittal sections of gill filament and expressed per millimeter of primary filament. Mean numbers of primary and secondary immunoreactive chloride cells for each group were obtained using the means calculated from each fish. Due to the uneven distribution of chloride cells in the gill, an entire piece of gill arch was sectioned, and images were randomly selected from 10 of the resulting sagittal sections. Cell area (μm^2/cell), shape factor, and staining intensity were also obtained from primary and secondary immunoreactive chloride cells. Shape factor is defined as $4\pi A/P^2$ (with A and P being area and perimeter, respectively), with values close to one indicating a round shape and less than one a more elongated shape. Immunoreactive cell staining intensity is measured as average 8-bit gray scale. To

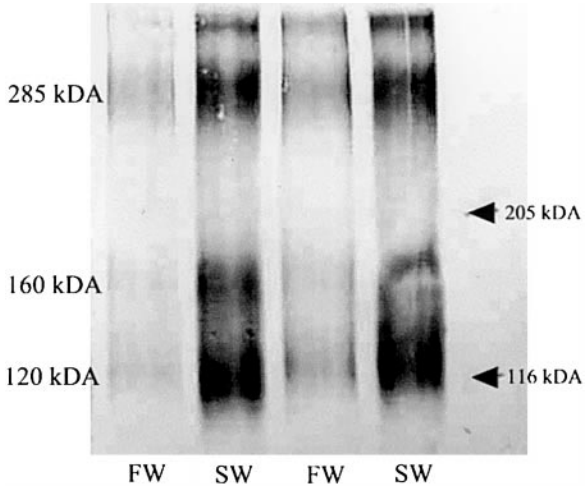

Fig. 1. Western blot of the Na^+-K^+-$2Cl^-$ cotransporter from freshwater (FW; *lanes 1* and *3*) and seawater-acclimated (SW; *lanes 2* and *4*) Atlantic salmon parr. The Western blot was probed with the T4 monoclonal primary antibody and 3 immunoreactive bands centered at 285, 160 and 120 kDa were obtained. Standards are marked (arrowheads) at 205 and 116 kDa.

standardize for differences in background staining intensity among images, background 8-bit gray scale was subtracted from the average 8-bit gray scale values from each immunoreactive cell. Fifty primary and fifty secondary immunoreactive chloride cells were analyzed from a minimum of five sagittal sections of gill filament from each fish. Fewer immunoreactive chloride cells on the secondary lamellae were analyzed from seawater-acclimated parr because fewer cells were present on the secondary lamellae. Means for each group were calculated using the means from individual fish. Cell number, size, shape factor, and staining intensities were obtained using MetaMorph 4.1.2 (Universal Imaging 1992–2000).

Data analysis. For salinity acclimation, data were analyzed using the Student's *t*-test or Mann-Whitney *U* test when appropriate. The Mann-Whitney *U* test was also used to compare plasma ion levels (Na^+ and Cl^-) in seawater-challenged juvenile Atlantic salmon in March and May. Analyses of the effects of smolting were conducted using a one-way analysis of variance or the Kruskal-Wallis test on ranks when the assumption of normality was not attained. Multiple comparisons were made using Tukey's honestly significant difference test. To establish the relationship between gill Na^+-K^+-$2Cl^-$ cotransporter abundance and Na^+-K^+-ATPase activity, a simple linear regression was performed. All statistical analyses were deemed significant at the $\alpha = 0.05$ level and conducted using Sigma Stat 2.0 (Jandel).

RESULTS

Characterization and localization of the gill Na^+-K^+-$2Cl^-$ cotransporter. Western blots of Atlantic salmon gill tissue membrane preparations revealed three broadly stained bands with molecular masses centered at 285, 160, and 120 kDa when probed with the T4 anti- Na^+-K^+-$2Cl^-$ cotransporter antibody (Fig. 1). On enzymatic deglycosylation, all three bands shifted downward with final masses of 230, 127, and 93 kDa. When staining intensity was low on Western blots, only the upper band was visible.

Immunoreactivity of the Na^+-K^+-$2Cl^-$ cotransporter was localized primarily to large, columnar cells on the primary gill filament of seawater-acclimated Atlantic salmon parr, and Na^+-K^+-ATPase was immunolocalized to these same cells (Fig. 2*A*). On the basis of size, location, and colocalization with Na^+-K^+-ATPase, Na^+-K^+-$2Cl^-$ cotransporter immunoreactivity occurred in chloride cells. In freshwater-acclimated parr, the Na^+-K^+-$2Cl^-$ cotransporter was also localized to chloride cells along with Na^+-K^+-ATPase. There were, how-

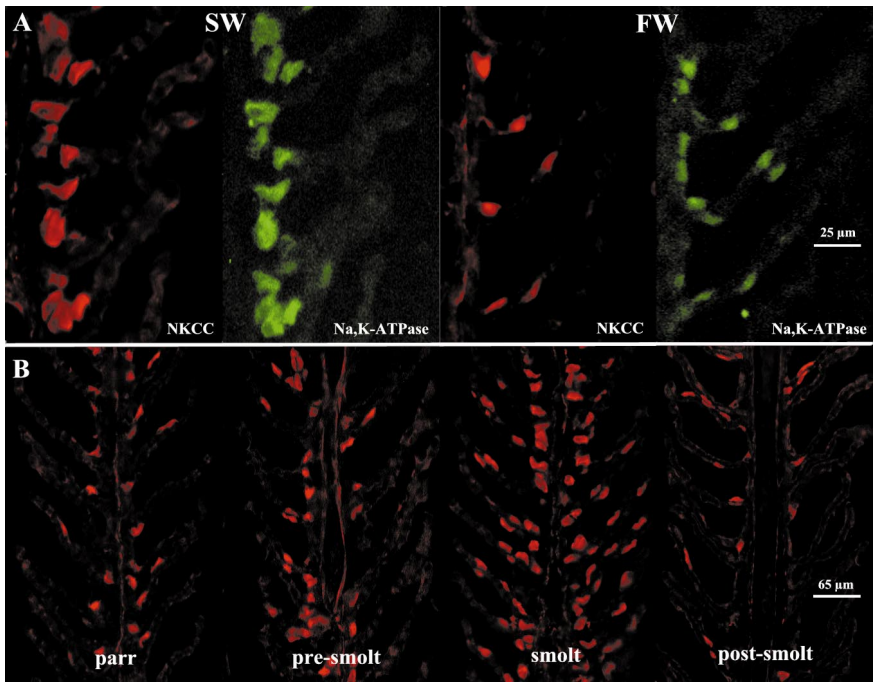

Fig. 2. Colocalization of the Na^+-K^+-$2Cl^-$ cotransporter (NKCC; red) and Na^+-K^+-ATPase (green) to gill chloride cells of FW and SW Atlantic salmon parr (*A*). Na^+-K^+-$2Cl^-$ cotransporter immunoreactivity in the gill during the parr-smolt transformation (*B*; parr in May, presmolts in February, smolts in May, and postsmolts in June).

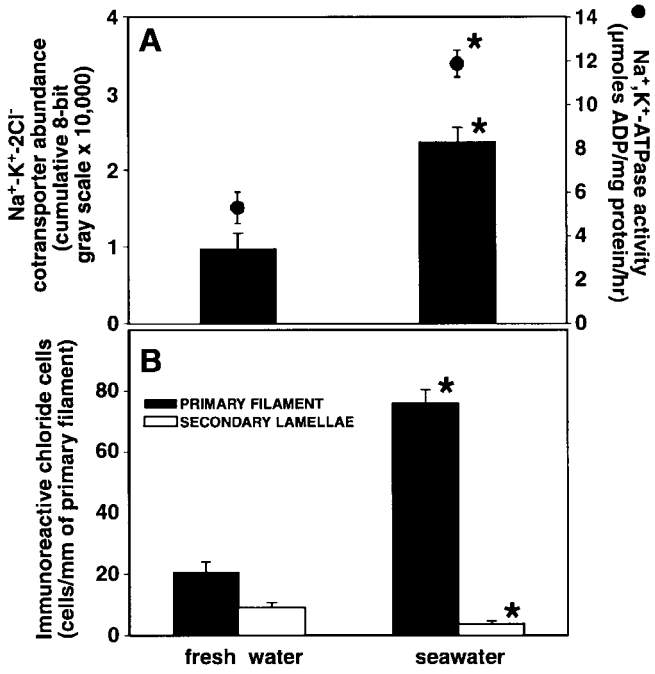

Fig. 3. Gill Na^+-K^+-$2Cl^-$ cotransporter abundance (solid bars; $n = 8$, means + SE) and gill Na^+-K^+-ATPase activity (μmol ADP·mg $protein^{-1}$·h^{-1}, ●; $n = 16$, means ± SE) in FW- and SW-acclimated Atlantic salmon parr (*A*). *Significantly different, $P < 0.05$. Student's *t*-test and Mann-Whitney *U* test for Na^+-K^+-$2Cl^-$ cotransporter abundance and Na^+-K^+-ATPase activity, respectively. Na^+-K^+-$2Cl^-$ cotransporter immunoreactive chloride cell number (cells/mm of primary filament) on the primary filament and secondary lamellae of FW- and SW-acclimated Atlantic salmon parr (*B*). *Significantly different, $P < 0.05$, Student's *t*-test.

ever, chloride cells only immunoreactive for Na^+-K^+-ATPase present on the primary filament and secondary lamellae. No detectable staining occurred in the other major cell types of the gill epithelia (pavement, pillar, and mucous cells) or in red blood cells or cartilage. Immunoreactive staining appeared to be distributed evenly throughout chloride cells, except for the absence of staining in nuclei.

Salinity acclimation. Gill Na^+-K^+-$2Cl^-$ cotransporter abundance, as measured by cumulative 8-bit gray scale from all three bands on Western blots, increased 2.5-fold in parr acclimated to seawater (Fig. 3*A*). The same molecular mass bands (285, 160, and 120 kDa) were observed in gill tissue from freshwater- and seawater-acclimated salmon (Fig. 1). Gill Na^+-K^+-ATPase activity increased 2.3-fold in seawater-acclimated parr (Fig. 3*A*).

After seawater transfer, Na^+-K^+-$2Cl^-$ cotransporter immunoreactive chloride cells on the primary filament increased 3.6-fold in number, whereas cells on the secondary lamellae decreased by a factor of 2.5 (Fig. 3*B*). The size of immunoreactive chloride cells on the primary filament and secondary lamellae increased approximately twofold after seawater transfer (Table 1). There were no differences in the shape, as measured by shape factors, or staining intensities of primary and secondary immunoreactive chloride cells among freshwater- and seawater-acclimated parr.

Smolting. Seawater-challenged juvenile Atlantic salmon in May had significantly lower ($n = 7$, $P < 0.05$, Mann-Whitney *U* test) plasma Na^+ (180.6 ± 3.4 mM) and Cl^- (160.9 ± 3.7 mM) levels than fish sampled in March (Na^+, 194.6 ± 3.8 mM; Cl^-, 178.5 ± 4.8 mM), indicating higher salinity tolerance among fish in May. In May, high levels of gill Na^+,K^+-ATPase activity (12.1 ± 0.42 μmol ADP·mg $protein^{-1}$·h^{-1}), the appearance of silvering and darkened fin margins, and higher salinity tolerance confirmed that the fish were smolts.

Gill Na^+-K^+-$2Cl^-$ cotransporter abundance, as measured by cumulative 8-bit gray scale from all three bands on Western blots, was low in presmolts (February), increased 3.3-fold in smolts (May), and declined 85.8% in postsmolts by June (Fig. 4*A*). Gill Na^+-K^+-$2Cl^-$ cotransporter abundance of parr sampled in May was 77.5% less than in smolts. Changes in gill Na^+-K^+-$2Cl^-$ cotransporter abundance paralleled changes observed in gill Na^+-K^+-ATPase activity. Linear regression analysis of Na^+-K^+-$2Cl^-$ cotransporter abundance against Na^+-K^+-ATPase activity indicated a significant and positive correlation ($n = 32$, $P < 0.001$, $r^2 = 0.86$) between the relative abundance of both proteins. Gill Na^+-K^+-ATPase activity was low in presmolts, increased more than twofold in smolts, and declined in postsmolts. Gill Na^+-K^+-ATPase activity of parr in May was 41% of the activity in smolts.

When probed with the T4 anticotransporter antibody, the number of immunoreactive chloride cells on the primary filament increased threefold from presmolt to smolt, sharply declining (89.4%) to low levels in postsmolts (Figs. 2*B* and 4*B*). The number of immunoreactive chloride cells on the primary filament of parr did not differ from that of presmolts. The number of immunoreactive chloride cells on the secondary lamel-

Table 1. *Size, shape factor, and staining intensity of Na^+-K^+-$2Cl^-$ cotransporter IRCCs on the primary filament (1° IRCCs) and secondary lamellae (2° IRCCs) of FW- and SW-acclimated Atlantic salmon parr*

	Cell Area, μm^2		Cell Shape		Cell Staining Intensity	
	1° IRCCs	2° IRCCs	1° IRCCs	2° IRCCs	1° IRCCs	2° IRCCs
FW parr	59.2 ± 3.0	54.9 ± 4.7	0.65 ± 0.02	0.48 ± 0.02	62.5 ± 4.8	54.9 ± 4.7
SW parr	116.5 ± 5.8*	102.8 ± 13.7*	0.62 ± 0.01	0.50 ± 0.02	74.4 ± 4.0	65.3 ± 7.3

Values are means ± SE; $n = 7$ [$n = 5$ for 2° immunoreactive chloride cells (IRCCs) from saltwater (SW) parr]. *Significantly different, $P < 0.05$ (Student's *t*-test for cell size and shape, and Mann-Whitney *U* test for cell staining intensity). Shape factor is defined as $4\pi A/P^2$ (with A and P being area and perimeter, respectively) with values close to 1 indicating a round shape and less than 1 an elongate shape. FW, freshwater.

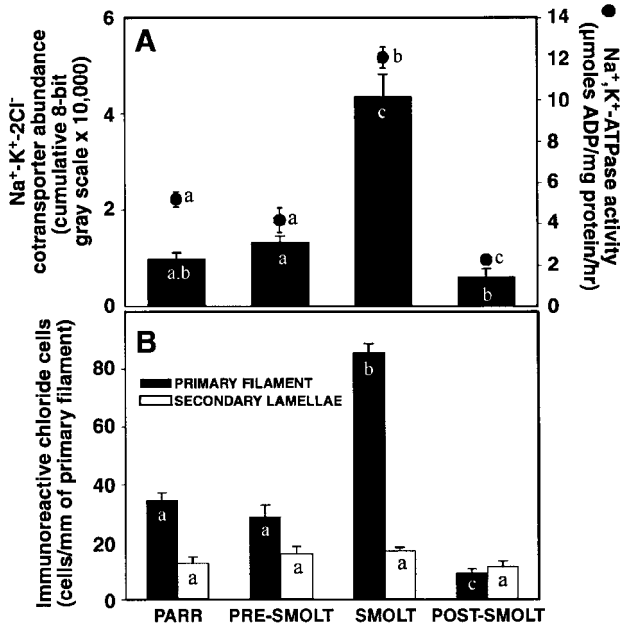

Fig. 4. Gill Na^+-K^+-$2Cl^-$ cotransporter abundance (solid bars; $n = 8$, mean + SE) and Na^+-K^+-ATPase activity (*A*; μmol ADP·mg $protein^{-1}$ $\cdot h^{-1}$, ●; $n = 8$, $n = 16$ for parr in May, mean ± SE), and the number of Na^+-K^+-$2Cl^-$ cotransporter immunoreactive chloride cells (*B*; cells/mm of primary filament) on the primary filament and secondary lamellae in Atlantic salmon parr (May), presmolts (February), smolts (May), and postsmolts (June). Different letters represent significant differences among groups. $P < 0.05$, Kruskal-Wallis procedure for gill Na^+-K^+-$2Cl^-$ cotransporter abundance and Na^+-K^+-ATPase activity and 1-way analysis of variance for immunoreactive chloride cell number. Multiple comparisons were made using Tukey's honestly significant difference test.

lae did not differ between parr, presmolt, smolt, and postsmolt.

The size of immunoreactive chloride cells on both the primary filament and secondary lamellae increased 1.5-fold from presmolt to smolt (Table 2). In postsmolts, immunoreactive chloride cells on the secondary lamellae were reduced to presmolt sizes, whereas cells on the primary filament remained enlarged. The size of immunoreactive chloride cells on both the primary filament and secondary lamellae of parr were the same as those observed in presmolts.

Chloride cells found on the secondary lamellae were more elongate than those found on the primary filament (shape factors of 0.451–0.493 and 0.613–0.671, respectively). Immunoreactive chloride cells on the primary filament of parr (May) were more round (shape factor of 0.671) than in presmolts, smolts, and postsmolts (0.613, 0.626, and 0.613, respectively). The shape of cells on the secondary lamellae did not differ with developmental stage.

Staining intensities of immunoreactive chloride cells on the primary filament and secondary lamellae were high in presmolts and smolts and reduced in postsmolts. Immunoreactive chloride cell (primary filament and secondary lamellae) staining intensities did not differ among parr and smolts. Immunoreactive chloride cells on the primary filament and secondary lamellae were stained with similar intensity (staining intensities of 57.1–76.7 and 49.1–73.4, respectively).

DISCUSSION

This is the first published study to identify, characterize, and localize the Na^+-K^+-$2Cl^-$ cotransporter in the gill of any teleost fish. The T4 antibody has been shown to recognize both the absorptive and secretory isoforms of the cotransporter from 23 different cell types among a wide variety of species (23). This includes rectal gland tissue from one elasmobranch fish, the spiny dogfish (*S. acanthias*). With the use of the T4 antibody and Western blots in this study, Atlantic salmon gill contained three bands with molecular masses centered at 285, 160, and 120 kDa (Fig. 1). The Na^+-K^+-$2Cl^-$ cotransporter has been shown to exhibit a wide variety of sizes depending on the species and/or tissue: 195 kDa in the shark rectal gland (22), 180 kDa in the kidney of winter flounder, *P. americanus* (39), and 164 kDa in the human colon (23). In the gills of killifish (*F. heteroclitus*), the Na^+-K^+-$2Cl^-$ cotransporter is ~190 kDa large, and between 210 and 260 kDa in the gills of rainbow trout, *Onchorynchus mykiss* (B. Forbush III, personal communication). Similar sizes for the upper band isolated on Western blots in this study and for the Na^+-K^+-$2Cl^-$ cotransporter in trout (a familial relative) further validate the isolation of the Atlantic salmon gill Na^+-K^+-$2Cl^-$ cotransporter.

Studies characterizing the Na^+-K^+-$2Cl^-$ cotransporter on Western blots have reported enzymatic deglycosylation of the protein (22, 23, 32). These studies identify a shift of 20–60 kDa on deglycosylation depending on the tissue source. In this study, the three

Table 2. *Changes in the size, shape factor, and staining intensity of Na^+-K^+-$2Cl^-$ cotransporter IRCCs on the primary filament (1° IRCCs) and secondary lamellae (2° IRCCs) in parr (May), presmolts (February), smolts (May), and postsmolts (June)*

	Cell Area, μm²		Cell Shape		Cell Staining Intensity	
	1° IRCCs	2° IRCCs	1° IRCCs	2° IRCCs	1° IRCCs	2° IRCCs
Parr	70.4 ± 2.8*	57.7 ± 2.8*	0.671 ± 0.008†	0.493 ± 0.01	57.1 ± 2.5*‡	49.1 ± 2.9*‡
Presmolts	71.3 ± 3.5*	59.3 ± 2.1*	0.613 ± 0.007*	0.485 ± 0.01	76.7 ± 3.4†	73.4 ± 5.0†
Smolts	107.0 ± 5.1†	83.5 ± 2.6†	0.626 ± 0.01*	0.482 ± 0.01	67.5 ± 3.1*†	64.1 ± 2.7*†
Postsmolts	99.8 ± 3.9†	64.1 ± 2.5*	0.613 ± 0.01*	0.451 ± 0.01	61.9 ± 2.2‡	55.9 ± 1.5‡

Values are means ± SE; $n = 8$. Different symbols indicate significant differences among groups at a given time point ($P < 0.05$). For cell size and shape, tests were conducted using a 1-way analysis of variance, and the nonparametric Kruskal-Wallis test was used for cell staining intensity. Multiple comparisons were made using Tukey's honestly significant difference test.

bands shifted down to 230, 127, and 93 kDa, respectively, when deglycosylated. This indicates a similar pattern of glycosylation for the protein isolated on Western blots in this study and provides additional evidence that the isolated protein is the Na^+-K^+-$2Cl^-$ cotransporter. The band at 285 kDa likely represents the glycosylated form, and the band at 230 kDa represents the core mass of the cotransporter. The lower molecular mass bands (160 and 120 kDa) likely represent degradation products. Three bands (180, 110–70, and 50 kDa) corresponding to the Na^+-K^+-$2Cl^-$ cotransporter in winter flounder intestine have previously been reported (39). The large amount of degradation present on Western blots may be due to the protein being in different stages of glycosylation. An alternative explanation, however, is that the lipophilic nature of the Na^+-K^+-$2Cl^-$ cotransporter may affect its migration through SDS-PAGE gels.

The Na^+-K^+-$2Cl^-$ cotransporter was localized specifically to chloride cells and was present at low or nondetectable levels in other cell types in the gill (Fig. 2*A*). Positively stained cells were identified as chloride cells on the basis of their colocalization with Na^+-K^+-ATPase, size, morphology, and location within the gill. The current model of seawater chloride cells includes both the Na^+-K^+-$2Cl^-$ cotransporter and Na^+-K^+-ATPase on the basolateral surface of the cell. Except for the nucleus, Na^+-K^+-$2Cl^-$ cotransporter immunoreactivity occurred throughout chloride cells, and immunoreactivity was similar to that exhibited by Na^+-K^+-ATPase. Previous work using [^{3}H]ouabain has localized Na^+-K^+-ATPase to the tubular system of chloride cells (17). Although the tubular system spreads throughout the chloride cell, it is contiguous with the basolateral surface. A similar even distribution of Na^+-K^+-ATPase-specific anthroylouabain staining in chloride cells of the tilapia (*Oreochromis mossambicus*) and the long-jawed mudsucker (*Gillichthys mirabilis*) has been described (26). Similar immunocytochemical staining of the Na^+-K^+-$2Cl^-$ cotransporter and Na^+-K^+-ATPase in this study suggests that the cotransporter is also present on the basolateral surface of chloride cells. Further research at the electron microscopic level will be necessary to confirm this.

The upregulation of the Na^+-K^+-$2Cl^-$ cotransporter during seawater acclimation and the localization of this transport protein to chloride cells is further evidence for the role of this protein in ion secretion by the gill. Seawater acclimation of Atlantic salmon parr increased gill Na^+-K^+-$2Cl^-$ cotransporter abundance and Na^+-K^+-ATPase activity (Fig. 3*A*). Similarly, the number (Fig. 3*B*) and size (Table 1) of Na^+-K^+-$2Cl^-$ cotransporter immunoreactive chloride cells on the primary filament, and the size of immunoreactive chloride cells on the secondary lamellae increased significantly after seawater transfer. Although this is the first study to quantify Na^+-K^+-$2Cl^-$ cotransport protein in the gill, other studies in a large number of teleosts have demonstrated increases in gill Na^+-K^+-ATPase activity after seawater transfer (see reviews, Refs. 7, 15, 24, 28). Gill Na^+-K^+-2Cl cotransporter abundance increased 2.5-fold after seawater acclimation, and gill Na^+,K^+-ATPase activity experienced a similar 2.5-fold increase (Fig. 3*A*). The strong correlation ($P < 0.001$, $r^2 = 0.86$) between the gill Na^+-K^+-$2Cl^-$ cotransporter and Na^+-K^+-ATPase suggests a possible mechanistic link between these two transport proteins. A similar association between the abundance of Na^+-K^+-$2Cl^-$ cotransporter and Na^+-K^+-ATPase has been shown in other ion-transporting tissues (23). Because the cotransport of sodium and chloride across the basolateral surface of seawater chloride cells is dependent on the sodium gradient created by Na^+-K^+-ATPase, parallel regulation of these proteins during seawater acclimation is not surprising.

Gill Na^+-K^+-$2Cl^-$ cotransporter abundance increased during the developmental process of smolting, coinciding with increased gill Na^+-K^+-ATPase activity and increased salinity tolerance (Fig. 4*A*). Other studies examining smolting in salmonids have reported preparatory changes in the osmoregulatory physiology of salmonids in the spring associated with increased salinity tolerance. These preparatory changes include increased gill Na^+-K^+-ATPase activity (21, 38) and chloride cell number and size (18). In this study, smolts had increased numbers of Na^+-K^+-$2Cl^-$ cotransporter immunoreactive chloride cells on the primary filament (Fig. 4*B*) and enlarged immunoreactive chloride cells on the primary filament and secondary lamellae (Table 2). The number of immunoreactive chloride cells on the secondary lamellae did not change throughout the developmental period of smolting. The increased levels of Na^+-K^+-$2Cl^-$ cotransporter, Na^+-K^+-ATPase, and numbers of chloride cells in Atlantic salmon gills are likely to be underlying causes of the increased seawater tolerance observed during smolting. Na^+-K^+-$2Cl^-$ cotransporter immunoreactive chloride cells on the primary filament of parr were more round than immunoreactive chloride cells of presmolts, smolts, and postsmolts (Table 2). It has been observed that β-chloride cells, which are more prevalent in freshwater parr than smolts, are more rounded than seawater α-chloride cells (36). The staining intensities of Na^+-K^+-$2Cl^-$ cotransporter immunoreactive chloride cells (primary and secondary) were elevated in presmolts and smolts, indicating more protein per cross-sectional area. After smolting, gill Na^+-K^+-$2Cl^-$ cotransporter abundance and Na^+-K^+-$2Cl^-$ cotransporter immunoreactive chloride cell number (primary filament), size (secondary lamellae), and staining intensities (primary filament and secondary lamellae) were reduced to levels that were comparable to those seen in parr (May). Many physiological changes associated with smolting, including increased gill Na^+-K^+-ATPase activity are lost after smolting, resulting in a loss of hypoosmoregulatory ability in postsmolts (29).

Although there is strong evidence for the role of the Na^+-K^+-$2Cl^-$ cotransporter in ion secretion, the presence of this protein in gill chloride cells of freshwater-acclimated fish is less easily explained (Fig. 1). Atlantic salmon parr can tolerate gradual increases in environmental salinity (3). The presence of the Na^+-K^+-$2Cl^-$

cotransporter may reflect the euryhaline life history of Atlantic salmon and indicate a moderate level of readiness for seawater entry. The concentration of the Na^+-K^+-$2Cl^-$ cotransport protein in chloride cells may also serve a physiological function in freshwater. Freshwater chloride cells have been implicated in ion uptake, calcium uptake, and acid-base metabolism (see Ref. 35). However, the most widely accepted models for these functions include Na^+-K^+-ATPase but not the Na^+-K^+-$2Cl^-$ cotransporter. The presence of Na^+-K^+-$2Cl^-$ cotransporter immunoreactivity in some but not all chloride cells exhibiting Na^+-K^+-ATPase immunoreactivity in freshwater-acclimated parr (Fig. 2*A*) suggests that the cotransporter plays a less critical role than Na^+-K^+-ATPase in ion absorption. Rather than a direct role, the greater concentration of the Na^+-K^+-$2Cl^-$ cotransporter in chloride cells in freshwater may reflect the cell's increased demand for volume regulation as an active ion transport cell.

Chloride cells on the primary filament increase in size and number after seawater transfer of most teleost fish (see reviews, 19, 20, 28). An increase in the number (Table 1) and size (Fig. 3*B*) of immunoreactive chloride cells on the primary filament was observed in this study, whereas chloride cells on the secondary lamellae declined in number. It has been demonstrated that chloride cells on the secondary lamellae of chum salmon (*Oncorhynchus keta*) fry are greatly reduced after seawater transfer (40), whereas they are totally absent in seawater-acclimated Atlantic salmon smolts (36). Chloride cells on the secondary lamellae proliferate during exposure to ion-poor water (1). These data suggest that chloride cells on the primary filament are involved in ion secretion, whereas chloride cells on the secondary lamellae take up ions. Because the current model of the freshwater chloride cell lacks an Na^+-K^+-$2Cl^-$ cotransporter, if chloride cells on the secondary lamellae are solely involved in ion uptake, we would expect to see low levels of the Na^+-K^+-$2Cl^-$ cotransporter in secondary lamellar chloride cells. This in fact was not the case, because chloride cells on the primary filament and secondary lamellae were stained with similar intensity (Tables 1 and 2). Furthermore, in seawater-acclimated parr, immunoreactive chloride cells on the primary filament (116.5 ± 5.8 μm^2) and secondary lamellae (102.8 ± 13.7 μm^2) were similar in size. The present study, therefore, does not provide evidence that there are two functionally distinct chloride cells on the primary filament and secondary lamellae. It is possible that in Atlantic salmon there is a single chloride cell type that provides an absorptive or secretory role (bifunctional) depending on development and the salinity of the external environment. By tracking in vivo sequential changes in individual chloride cells it was recently shown that individual chloride cells in the yolk sac membrane of tilapia (*O. mossambicus*) embryos and larvae increase in size after freshwater to seawater transfer (11), suggesting that individual cells can change from ion uptake to ion secretion, and are therefore bifunctional.

The current study demonstrates that the Na^+-K^+-$2Cl^-$ cotransporter is present in gill chloride cells of Atlantic salmon and is upregulated after seawater acclimation and during the developmental process of smolting. Changes in gill Na^+-K^+-ATPase were parallel to changes in the Na^+-K^+-$2Cl^-$ cotransporter, suggesting a mechanistic link between the proteins in ion secretion by gill chloride cells. These observations provide the first direct support for the inclusion of the Na^+-K^+-$2Cl^-$ cotransporter in the current models of chloride cell ion secretion by the gills of teleost fish.

We thank J. Kunkel for methodological assistance and Dr. K. Ura for generously providing the antibody against Na^+-K^+-ATPase. G. B. Zydlewski made many helpful comments in review of the manuscript.

Present addresses: J. Zydlewski, Abernathy Fish Technology Center, US Fish and Wildlife Service, Longview, WA 98632; R. Pelis, University of Connecticut, BBS#4, Rm. 021, Physiology and Neurobiology, U-4156, 3107 Horsebarn Hill Rd., Storrs, CT 06269-4156.

REFERENCES

1. **Avella M, Masoni A, Bornancin M, and Mayer-Gostan N.** Gill morphology and sodium influx in the rainbow trout *(Salmo gairdneri)* acclimated to artificial freshwater environments. *J Exp Zool* 24: 159–169, 1987.
2. **Davis MS and Shuttleworth TJ.** Peptidergic and adrenergic regulation of electrogenic ion transport in isolated gills of the flounder (*Platichthys flesus* L). *J Comp Physiol [A]* 155: 471–478, 1985.
3. **Duston J.** Effect of salinity on survival and growth of Atlantic salmon (*Salmo salar*) parr and smolts. *Aquaculture* 121: 115–124, 1994.
4. **Ecelbarger CA, Terris J, Hoyer JR, Nielsen S, Wade JB, and Knepper M.** Localization and regulation of the rat renal Na^+-K^+-$2Cl^-$ cotransporter, BSC-1. *Am J Physiol Renal Fluid Electrolyte Physiol* 271: F619–F628, 1996.
5. **Epstein FH, Katz AI, and Pickford GE.** Sodium- and potassium-activated adenosine triphosphatase of gills: role in adaptation of teleosts to salt water. *Science* 156: 1245–1247, 1967.
6. **Eriksson O, Mayer-Gostan N, and Wistrand PJ.** The use of fish opercular epithelium as a model tissue for studying intrinsic activities of loop diuretics. *Acta Physiol Scand* 125: 55–56, 1985.
7. **Evans DH, Piermarini PM, and Potts WTW.** Ionic transport in the fish gill epithelium. *J Exp Zool* 283: 641–652, 1999.
8. **Fosket JK and Scheffey C.** The chloride cell: definitive identification as the salt-secretory cell in teleosts. *Science* 215: 164–166, 1982.
9. **Frizzel RA, Halm DR, Musch MW, Stewart CP, and Field M.** Potassium transport by flounder intestinal mucosa. *Am J Physiol Renal Fluid Electrolyte Physiol* 246: F946–F951, 1984.
10. **Ginns SM, Knepper MA, Ecelbarger CA, Terris J, He X, Coleman RA, and Wade JB.** Immunolocalization of the secretory isoform of Na-K-Cl cotransporter in rat renal intercalated cells. *J Am Soc Nephrol* 7: 2533–2542, 1996.
11. **Hiroi J, Kaneko T, and Tanaka M.** In vivo sequential changes in chloride cell morphology in the yolk-sac membrane of Mozambique tilapia (*Oreochromis mossambicus*) embryos and larvae during seawater adaptation. *J Exp Biol* 202: 3485–3495, 1999.
12. **Hoar WS.** Smolt transformation: evolution, behavior, and physiology. *J Fish Res Board Can* 33: 1234–1252, 1976.
13. **Hootman SR and Philpott CW.** Ultracytochemical localization of Na^+, K^+-activated ATPase in chloride cells from the gills of a euryhaline teleost. *Anat Rec* 193: 99–130, 1979.
14. **Hossler FE.** Gill arch of the mullet, *Mugil cephalus*. III. Rate of response to salinity change. *Am J Physiol Regulatory Integrative Comp Physiol* 238: R160–R164, 1980.
15. **Karnaky KJ.** Structure and function of the chloride cells of *Fundulus heteroclitus* and other teleosts. *Am Zool* 26: 209–224, 1986.

16. **Karnaky KJ, Degnan KJ, and Zadunaisky JA.** Chloride transport across isolated opercular epithelium of killifish: a membrane rich in chloride cells. *Science* 195: 203–205, 1977.
17. **Karnaky KJ, Kinter LB, Kinter WB, and Stirling CE.** Teleost chloride cell. II. Autoradiographic localization of gill Na,K-ATPase in killifish *Fundulus heteroclitus* adapted to low and high salinity environments. *J Cell Biol* 70: 157–177, 1976.
18. **Langdon JS and Thorpe JE.** The ontogeny of smoltification: developmental patterns of gill Na^+/K^+-ATPase, SDH, and chloride cells in juvenile Atlantic salmon, *Salmo salar* L. *Aquaculture* 45: 83–96, 1985.
19. **Laurent P and Dunel S.** Morphology of gill epithelia in fish. *Am J Physiol Regulatory Integrative Comp Physiol* 238: R147–R159, 1980.
20. **Laurent P and Perry SF.** Environmental effects on fish gill morphology. *Physiol Zool* 64: 4–25, 1991.
21. **Lubin RT, Rourke AW, and Saunders RL.** Influence of photoperiod on the number and ultrastructure of gill chloride cells of the Atlantic salmon (*Salmo salar*) before and during smoltification. *Can J Fish Aquat Sci* 48: 1302–1307, 1991.
22. **Lytle C, Xu J, Biemesderfer D, Haas M, and Forbush B III.** The Na-K-Cl cotransport protein of shark rectal gland. *J Biol Chem* 267: 25428–25437, 1992.
23. **Lytle C, Xu J, Biemesderfer D, and Forbush B III.** Distribution and diversity of Na-K-Cl cotransport proteins: a study with monoclonal antibodies. *Am J Physiol Cell Physiol* 269: C1496–C1505, 1995.
24. **Marshall WS and Bryson SE.** Transport mechanisms of seawater teleost chloride cells: an inclusive model of a multifunctional cell. *Comp Biochem Physiol* 119A: 97–106, 1998.
25. **Matthews JB, Smith JA, Tally KJ, Awtrey CS, Nguyen HV, Rich J, and Madara JL.** Na-K-2Cl cotransport in intestinal epithelial cells—influence of chloride efflux and F-actin on regulation of cotransporter activity and bumetanide binding. *J Biol Chem* 269: 15703–15709, 1994.
26. **McCormick SD.** Fluorescent labelling of Na^+,K^+-ATPase in intact cells by use of a fluorescent derivative of ouabain: salinity and teleost chloride cells. *Cell Tissue Res* 260: 529–533, 1990.
27. **McCormick SD.** Methods for non-lethal gill biopsy and measurement of Na^+,K^+-ATPase activity. *Can J Fish Aquat Sci* 50: 656–658, 1993.
28. **McCormick SD.** Hormonal control of gill Na^+,K^+-ATPase and chloride cell function. In: *Fish Physiology, Ionoregulation: Cellular and Molecular Approaches*, edited by Wood CM and Shuttleworth TJ. NY: Academic, 1995, vol. 14, p. 285–315.
29. **McCormick SD, Hansen LP, Quinn TP, and Saunders RL.** Movement, migration, and smolting of Atlantic salmon (*Salmo salar*). *Can J Fish Aquat Sci* 55: 77–92, 1998.
30. **McCormick SD and Saunders RL.** Preparatory physiological adaptations for marine life in salmonids: osmoregulation, growth and metabolism. *Am Fish Soc Symp* 1: 211–229, 1987.
31. **McCormick SD, Saunders RL, Henderson EB, and Harmon PR.** Photoperiod control of parr-smolt transformation in Atlantic salmon (*Salmo salar*): changes in salinity tolerance, gill Na^+,K^+-ATPase activity, and plasma thyroid hormones. *Can J Fish Aquat Sci* 44: 1462–1468, 1987.
32. **O'Donnell ME, Martinez A, and Sun D.** Endothelial Na-K-Cl cotransport regulation by tonicity and hormones: phosphorylation of cotransport protein. *Am J Physiol Cell Physiol* 269: C1513–C1523, 1995.
33. **O'Grady SM, Palfrey HC, and Field M.** Na-K-Cl cotransport in winter flounder intestine and bovine outer medulla [^{3}H]bumetanide binding and effects of furosemide analogues. *J Membr Biol* 96: 11–18, 1987.
34. **O'Grady SM, Musch MW, and Field M.** Stoichiometry and ion affinities of the Na-K-Cl cotransport system in the intestine of the winter flounder (*Pseudopleuronectes americanus*). *J Membr Biol* 91: 33–41, 1986.
35. **Perry SF.** Relationships between branchial chloride cells and gas transfer in freshwater fish. *Comp Biochem Physiol* 119A: 9–16, 1998.
36. **Pisam M, Prunet P, Boeuf G, and Rambourg A.** Ultrastructural features of chloride cells in the gill epithelium of the Atlantic salmon, *Salmo salar*, and their modifications during smoltification. *Am J Anat* 183: 235–244, 1988.
37. **Richman HAI, Tai De Diaz S, Nishioka RS, Prunet P, and Bern HA.** Osmoregulatory and endocrine relationships with chloride cell morphology and density during smoltification in coho salmon (*Oncorhynchus kisutch*). *Aquaculture* 60: 265–285, 1987.
38. **Saunders RL and Henderson EB.** Changes in gill ATPase activity and smolt status of Atlantic salmon (*Salmo salar*). *J Fish Res Board Can* 35: 1542–1546, 1978.
39. **Suvitayavat W, Dunham PB, Haas M, and Rao MC.** Characterization of the proteins of the intestinal Na^+-K^+-$2Cl^-$ cotransporter. *Am J Physiol Cell Physiol* 267: C375–C384, 1994.
40. **Uchida K, Kaneko T, Yamauchi K, and Hirano T.** Morphometrical analysis of chloride cell activity in the gill filaments and lamellae and changes in Na^+,K^+-ATPase activity during seawater adaptation in chum salmon fry. *J Exp Zool* 276: 193–200, 1996.
41. **Ura K, Soyano K, Omoto N, Adachi S, and Yamauchi K.** Localization of Na^+,K^+-ATPase in tissues of rabbit and teleosts using an antiserum directed against a partial sequence of the α-subunit. *Zool Sci* 13: 219–227, 1996.
42. **Wu Q, Delpire E, Hebert SC, and Strange K.** Functional demonstration of Na^+-K^+-$2Cl^-$ cotransporter activity in isolated, polarized choroid plexus cells. *Am J Physiol Cell Physiol* 275: C1565–C1572, 1998.